

Heterogeneous Enzymatic Catalysts: Comparing Their Efficiency in the Production of Biodiesel from Alternative Oils †

Gabriel Orlando Ferrero *, Edgar Maximiliano Sánchez Faba and Griselda Alejandra Eimer *

¹ CITEQ-UTN-CONICET, Universidad Tecnológica Nacional, Facultad Regional Córdoba, Maestro López esq. Cruz Roja, Ciudad Universitaria, 5016, Córdoba, Argentina; edgar-sf_90@hotmail.com

² Affiliation 2; e-mail@e-mail.com

* Correspondence: gferrero@frc.utn.edu.ar (G.O.F.); geimer@frc.utn.edu.ar (G.A.E.)

† Presented at the 2nd International Electronic Conference on Catalysis Sciences—A Celebration of *Catalysts* 10th Anniversary, 15–30 October 2021; Available online: <https://eccs2021.sciforum.net/>.

Abstract: In this study, four heterogeneous enzymatic catalysts were synthesized: three from the immobilization of *Pseudomonas fluorescens* lipase (L_{pf}) on SBA-15, Ca/SBA-15, and Na / SBA-15, and one using the one-step coprecipitation technique, called LOBE (Low Ordered Biosilicified Enzyme). The physicochemical properties of these materials were determined by small-angle X-ray scattering (SAXS), Fourier Transform infrared spectroscopy (FT-IR), inductively coupled plasma atomic emission spectroscopy (ICP), and N₂ adsorption measurements. The biocatalysts activity was evaluated in the production of biodiesel with different oily raw materials. From these results, it was possible to infer that besides enzyme-metal-support synergistic effect (L_{pf} / Ca / SBA-15 or L_{pf} / Na / SBA-15), confinement effects that influences on the substrates diffusion or mass transfer depending the pore architecture is determining on the catalytic efficiency.

While the SBA-15 material presents one-dimensional channels, the LOBE biocatalyst has interconnected three-dimensional channels that favor the mixing of reactant phases (oil-alcohol) and interaction with active sites inside porous structure (as a nanoreactor). This characteristic would increase the specific activity of the LOBE biocatalyst approximately five times with respect to the other studied biocatalysts.

Keywords: biodiesel; non-edible oils; enzymatic immobilization; biocatalysis; renewable biofuel; alternative raw materials; sustainability

Citation: Lastname, F.; Lastname, F.; Lastname, F. Title. *Chem. Proc.* **2021**, *3*, x. <https://doi.org/10.3390/xxxxx>

Published: date

Publisher's Note: MDPI stays neutral with regard to jurisdictional claims in published maps and institutional affiliations.



Copyright: © 2021 by the authors. Submitted for possible open access publication under the terms and conditions of the Creative Commons Attribution (CC BY) license (<https://creativecommons.org/licenses/by/4.0/>).

1. Introduction

Global trends towards sustainability are driving demand for greener products with improved properties and new eco-friendly biomanufacturing. Biocatalyst engineering has the potential to effectively catalyze value-added bioconversion processes, improving the performance of enzymes for specific applications [1]. In this way, researchers use tools as synthetic biology and protein engineering to design new metabolic pathways and enzymes, respectively, to increase the enzyme performance or synthesize unnatural chemicals [2,3]. Another type of approach to improve enzyme performance is enzyme immobilization on porous materials [4]. This methodology increases the enzymatic activity since the protein can be distributed on a large surface, keeping them dispersed and preventing agglomerating in organic media, which reduces the number of exposed active sites [5,6]. Moreover, immobilization also increases the resistance to denaturing agents because, when the enzyme interacts with the support, its degrees of freedom are restricted [7]. The area, the size of the pores, and the nature of the support surface generally affect the enzyme activity. The specific area can be fully used only if the pore size is larger than the

enzyme size. Likewise, a total occupation of the pores by the enzymes can cause limitations in the diffusion of substrates and products within the pores [7]. The superficial and structural nature of the support can also modify directly or indirectly the enzyme activity. Thus, so-called confinement effects in porous materials can strongly affect diffusion, mass transfer and catalytic properties. In previous works, we describe that a modification of SBA-15 material with calcium or sodium has a synergic effect with the immobilized *Pseudomonas fluorescens* lipase, incrementing the transesterification activity. However, this material has also a disadvantage: due to its polar character, the glycerol obtained as a sub-product during the transesterification reaction strongly interacts with the modified supports, diffculting the mass transfer and decreasing the activity of the biocatalyst [6,8]. Methodologies for immobilizing enzymes include chemisorption, physical adsorption, and coprecipitation [9,10]. Chemisorption covalently binds enzymes to the support, leading to biocatalysts with high stability and performance. However, the non-specificity of the covalent bonds can produce enzyme denaturalization and decrease their activity. Physical adsorption is a rapid method for the immobilization of enzymes and is mainly based on electrostatic and hydrogen bond interactions between support-enzyme. This type of reversible immobilization reduces enzyme denaturation while increases its activity but, due to the weak interaction, enzyme leaching can occur. Coprecipitation consists of the protein immobilization on the support during its synthesis. In a single stage, an organic silicon precursor, a surfactant and an organic solvent are mixed with a buffer solution to produce the enzymatic mineralization. When silicon is used, the process is called biosilicification and provides exceptional enzymatic stability under drastic conditions [11].

At present, the method applied for biodiesel production is triglycerides transesterification with short-chain alcohol, which is divided into non-catalyzed reaction, inorganic-catalyzed reaction, and enzyme-catalyzed reaction. As a replacement for fossil fuels, biodiesel production using immobilized lipases is currently the focus of attention because enzyme immobilization avoids several problems, such as product contamination, effluent generation, and material handling problems, while allows repetitive and continuous use of the stabilized enzyme, the employment of raw material with high water and free fatty acids contents, effective control of reaction parameters and the use of mild reaction conditions (temperature of 30 °C and atmospheric pressure) [10,12–14]. The present work is aimed to investigate the role of the nature and the structure of the support in the activity of *Pseudomonas fluorescens* lipase. The synthesized biocatalysts were compared in the ethanolysis of different oils for biodiesel production. *Pseudomonas fluorescens* lipase was immobilized on the following materials: SBA-15 (pure silica), Ca/SBA-15 or Na/SBA-15 (metal surface-modified SBA-15), or by biosilicification in one step. As already described, the different functional groups on the surface of the material can affect the enzyme-support interactions and, therefore, the catalytic activity. However, the structure of the materials has been little studied in this regard. In this study, in addition to the nature of the supports, the influence of channel architecture on immobilized lipase catalytic efficiency for biodiesel production is analysed.

2. Materials and Methods

2.1. Materials

Pseudomonas fluorescens lipase (PFL, $\geq 20,000$ IU / g at 55 °C, pH 8.0) was purchased from Sigma-Aldrich Co. (St. Louis, USA). Sunflower oil (Cocinero, Molinos Río de la Plata S.A., Argentina), soybean oil (Sojola, Aceitera General Deheza S.A., Argentina), and ethanol 96% v/v (Porta Hnos. S.A., Argentina) were purchased at a local grocery store. Waste frying oil was obtained from different domestic sources and filtered before being used. Acid oil from soapstock (soybean) was generously gifted by a local company (Louis Dreyfus Company, Argentina). *Jatropha hieronymi* oil was kindly donated by Dr. Fracchia (CIRLAR-CONICET, La Rioja, Argentina). Other used reagents were: KH_2PO_4 , K_2HPO_4 , and KOH (Anedra), n-dodecylamine (Sigma-Aldrich, USA), n-hexane (analytical grade,

Merck), isopropyl alcohol (Fluka, USA), acetonitrile (analytical grade, Merck, USA), Pluronic 123 (Sigma-Aldrich, USA), hydrochloric acid (HCl) (analytical grade, Cicarelli), Tetraethyl orthosilicate (Aldrich, USA) and milliQ water. Syringe filters (polypropylene, 25 mm diameter and 0.2 micron pore size) were supplied by VWR (USA).

2.2. Synthesis and Modification of SBA-15

Pure SBA-15 was synthesized according Zhao et al. [15], metal-modified material were obtained using the wet impregnation method. Aqueous solutions of metal salt ((Ca(NO₃)₂) and NaNO₃) were used to reach theoretical metal loadings of 2.5 wt%. The SBA-15 host (0.75 g) was dispersed in the precursor solution at room temperature and then, the solvent (water) was removed slowly by rotary evaporation at 50 °C for 30 min. The resulting powder was dried at 60 °C and calcined for 8 h at 500 °C to obtain the modified material [16]. The supports were named Na/SBA-15 and Ca/SBA-15.

2.3. Materials Characterization

Small-angle X-ray scattering (SAXS) analysis was performed using a Xenocs XEUS 2.0 equipment provided with a Pilatus 100 K detector and CuK α radiation ($\lambda=0.154$ nm). Measures were made in the 2θ range of 0.3-11. The calcium and sodium contents in the synthesized catalysts were determined by Inductively Coupled Plasma Atomic Emission Spectroscopy (ICP) using a spectrophotometer VISTA-MPX CCD Simultaneous ICP-OES-VARIAN. The materials specific surface was determined using a Micromeritics Pulse Chemisorb 2700. Samples were previously dried using a N₂ flux for 3 h at 350 °C. The specific surface was determined by the Brunauer-Emmett-Teller (BET) method. The organic species on the biocatalyst were detected by infrared spectroscopy using a Thermo Scientific™ TQ Analyst™ 9.7 Software (Waltham, MA, USA) at room temperature. Spectra were recorded between 400 and 4600 cm⁻¹.

2.4. Immobilization of *Pseudomonas fluorescens* lipase

Pseudomonas fluorescens lipase were immobilized according Ferrero et al. [6]. The obtained hybrid materials were named L_{Pf}/SBA-15, L_{Pf}/Na/SBA-15, or L_{Pf}/Ca/SBA-15.

The biosilicification of the *Pseudomonas fluorescens* lipase were carry out according Ferrero et al. [17]. The hybrid material was named Low Ordered Biosilicificated Enzyme (LOBE).

The supernatant of the immobilizations was used to determine the protein content according to the Bradford method [18].

The amount of immobilized lipase was reported as "Protein Loading" and was determined according to the following equations:

$$\text{Actual protein (mg}_{\text{protein}}\text{)} = \text{Theoretical protein (mg)} - \text{Supernatant protein (mg)}, \quad (1)$$

$$\text{Protein Loading (mg}_{\text{protein}}\text{/g}_{\text{support}}\text{)} = \frac{\text{Actual protein (mg)}}{\text{Support (g)}}, \quad (2)$$

Immobilization efficiency was calculated as follows:

$$\text{Immobilization efficiency (\%)} = \frac{\text{Actual protein (mg)}}{\text{Theoretical protein mg}} \times 100, \quad (3)$$

2.5. Transesterification Reaction

The reaction was carried out in a screw vial placed in an orbital shaker at 80 rpm and 37 °C, with a sunflower oil/ethanol molar ratio of 1/4. The reaction was started when the biocatalyst was added (175 mg_{biocatalyst}/g_{oil} when L_{Pf}/SBA-15, L_{Pf}/Na/SBA-15, or L_{Pf}/Ca/SBA-15 was used or 125mg_{biocatalyst}/g_{oil} when LOBE was used) to the substrates mix. 50 mg_{enzyme}/g_{oil} were used to evaluated free enzymes. Samples were taken at different times, then, they were diluted to a volume of 4 mL with isopropanol, filtered with a 0.45 mm pore size filter, and analyzed by HPLC [19]. The "Enzymatic activity" and the "Specific activity" were calculated according to the following equations:

$$\text{Enzymatic activity (U)} = \frac{\text{Produced FAEE content (mg)}}{\text{Time (min)}}, \quad (4)$$

$$\text{Specific activity (U/g}_{\text{protein}}) = \frac{U}{\text{Actual protein (g)}}, \quad (5)$$

2.6. Chromatographic Analysis

The analyzes were performed using a Perkin Elmer HPLC with UV-vis detector of the 200 series equipped with a solvent delivery unit with a gradient of elution, a Vertex Plus (250 mm × 4.6 mm, 5 μm) Eurospher II 100-5 C18P column, the used software was TotalChrom, according Carvalho et al. [20]. All reactions were performed at least in duplicate and the results were expressed as mean values, with the percentage differences between them were always less than 5% of the mean.

3. Result and discussion

Main text paragraph (M_Text).

3.1. Catalysts Characterization

In this work, four enzymatic heterogeneous catalysts were used for biodiesel production. Three of them were obtained by the physical adsorption of the lipase on the pure synthesized material SBA-15 or the metal modified materials with sodium or calcium according to [6,19,21]. They were denominated $L_{PS}/SBA-15$, $L_{PS}/Na/SBA-15$ or $L_{PS}/Ca/SBA-15$ respectively. The fourth hybrid biocatalyst was obtained by enzymatic mineralization with an organic silicic precursor according to [17]. This technique, the biosilicification [22], provided the enzymatic heterogeneous catalyst in only one step denominated “Low Ordered Biosilicified Enzyme” (LOBE).

The chemical environment in which a peptide or protein exists influences its structure and stability. For this reason, the FT-IR technique was used to determine the structural characterization and the presence of proteins on the enzymatic heterogeneous catalysts [23].

The characteristic functional groups of free *Pseudomonas fluorescens* lipase can be observed in Figure 1a. The stretching vibrations of –OH groups, corresponding to moisture, became visible as a broad band between 3600 and 3200 cm^{-1} , which would be also masking the –N–H stretching vibrations. The bands at 2930 cm^{-1} and 2850 cm^{-1} are assigned to the stretching C–H vibrations of –CH₂ and –CH₃ groups, respectively. The typical stretching vibrations of carbonyl groups appear around 1700 cm^{-1} and stretching vibration of ≡C–O– is observed at 1180 cm^{-1} . Amide I and amide II, the most characteristic functional groups of the pure enzymes, are seen at 1645 cm^{-1} and 1542 cm^{-1} , respectively [24].

Figure 1 b, c, d, e, and f correspond to FT-IR spectra of the LOBE, $L_{Pf}/SBA-15$, $L_{Pf}/Na/SBA-15$, $L_{Pf}/Ca/SBA-15$, and SBA-15, respectively. The presence of water adsorbed on the material is observed at 3440 cm^{-1} , caused by the material hydrophilic character [25]. The band of ≡Si–O bond vibration at 1070 cm^{-1} and the signals among 800 cm^{-1} and 460 cm^{-1} confirm the siliceous presence [26]. Meanwhile, the Si–OH bending band that appears at 960 cm^{-1} , results less defined when the material is modified with Na and Ca, possibly due to the metal interaction with the support surface. The intensities and wavenumbers of amides bands in the enzymatic heterogeneous catalysts decrease, indicating that the immobilization of the lipase inside the silica matrix was successful [27]. Moreover, the presence of the amide I and amide II bands indicates that the enzyme secondary structure and bioactivity are conserved in the formed nanostructures [28]. Also, bands at 2930 cm^{-1} and 2850 cm^{-1} in the LOBE spectrum, assigned to (C–H) stretching of the saturated –CH₂ and –CH₃ groups, increase their intensity concerning the free enzyme due to the surfactant presence.

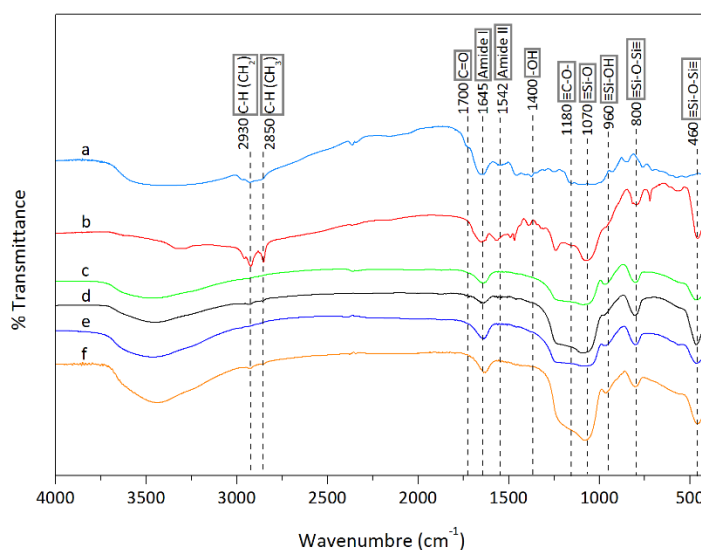


Figure 1. FT-IR spectra of lipase immobilized on the different supports: a) free lipase, b) LOBE, c) LPf/SBA-15, d) LPf/Na/SBA-15, e) LPf/Ca/SBA-15 and f) SBA-15.

In order to reach an adequate comparison between the different obtained enzymatic heterogeneous catalysts it is key analyzing the nature of the materials used to immobilize the enzyme measuring both structural and texture properties. Thus, Figure 2 b-d shows SAXS patterns of the pure SBA-15, Ca/SBA-15 and Na/SBA-15, which present three well-resolved peaks, corresponding to the diffraction of planes (1 0 0), (1 1 0), and (2 0 0) characteristic of the SBA-15 structure. These reflections are typical of a hexagonal ordered and unidimensional pore arrangement [15].

As it can be observed, after sodium and calcium incorporation, the periodic arrangement of SBA-15 remains. Meanwhile, the LOBE presents a different pattern, with two maxima peaks assigned to (2 1 1) and (2 2 0) reflections. These reflections and the ratio value d_{220}/d_{2110} (~ 0.87) are consistent with a tridimensional cubic structure similar to MCM-48 [29] (Figure 2d). It should be noted here that LOBE is already the hybrid biocatalyst obtained by enzymatic mineralization with an organic silicic precursor in only one step.

3.2. Performance of Enzymatic Heterogeneous Catalysts to Biodiesel Production

The production of FAEE from sunflower oil and bioethanol when employing the studied biocatalysts is shown in Figure 3. As it can be observed the highest FAEE contents are achieved after 48h of reaction for LOBE, LPf/Ca/SBA-15, and LPf/Na/SBA-15. Meanwhile, the LPf/SBA-15 and free lipase produced 83 wt% and 36 wt% (11% and 61% less biodiesel than the mentioned biocatalysts), respectively. The low activity of free lipase was due to the proteins aggregation phenomenon when they are in an organic solvent [29].

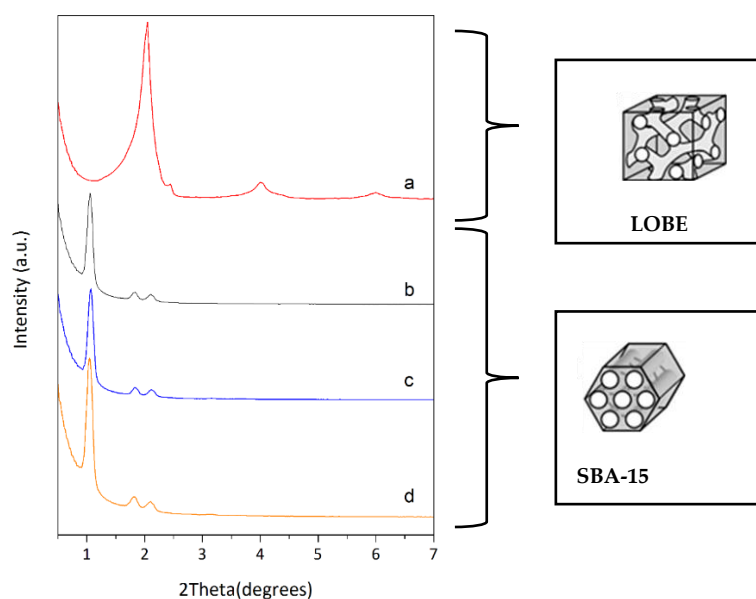


Figure 2. Small-angle X-ray scattering patterns of: a) LOBE, b) Na/ SBA-15, c) Ca/ SBA-15 and d) SBA-15.

However, when the lipase was immobilized on a mesoporous surface, such as $L_{PF}/SBA-15$, the activity markedly increased. As consequence of immobilization, the enzymes could be well dispersed on the material surface, improving the availability of active sites to carry out the reaction [6,21].

As it was mentioned in previous work, the presence of alkaline metals (sodium and calcium) produce a synergic effect enzyme-support, being responsible for the increase in the FAEE content [6].

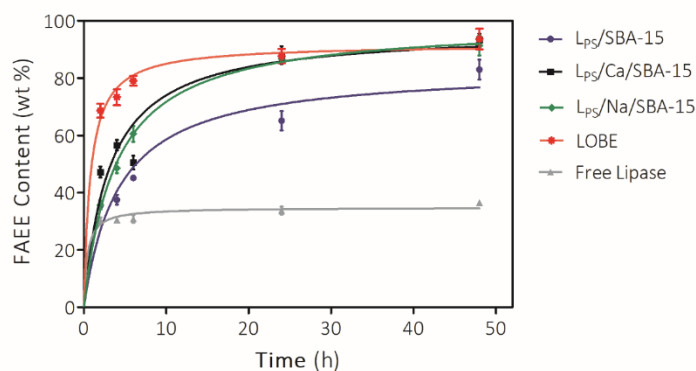


Figure 3. Evaluation of catalysts performance to produce FAEE. Reaction conditions: ethanol/oil molar ratio = 4/1; 125 mg of catalyst/g of oil; 37 °C and constant shaking (140 oscillations/min).

Since LOBE catalyst was synthesized by a different methodology (biosilicification), to compare the performance of the obtained biocatalysts from the several immobilization techniques and different supports, the protein loading, immobilization efficiency, enzymatic activity, and specific activity were determined (Table 1).

Table 1. Protein loading, Immobilization efficiency, Enzymatic activity, and specific activity of the synthesized biocatalysts.

Biocatalyst	Protein loading ($\text{mg}_{\text{protein}}/\text{g}_{\text{support}}$)	Immobilization efficiency (%)	Enzymatic activity (U)	Specific activity ($\text{U}/\text{g}_{\text{lipase}}$)
Free lipase	-	-	0,02	0,47
$L_{PF}/SBA-15$	392.00	98.00	0,05	0,92

$L_{PF}/Na/SBA-15$	389.92	97.48	0,06	1,24
$L_{PF}/Ca/SBA-15$	395.20	98.80	0,06	1,24
LOBE	66.85	96.88	0,06	7,29

As it is shown in Table 1, all biocatalysts present a good immobilization efficiency, greater than 96%. The specific activity of the lipase increases 1,96 times when the enzyme is immobilized in SBA-15. Meanwhile, if the siliceous support is modified with Na or Ca the specific activity enhances 2,64 times concerning free lipase, evidencing the aforementioned synergistic effect. The protein loading for LOBE is approximately 6 times lower than that for the rest of the biocatalysts; however, it has good enzymatic activity and the best specific activity (at least 5 times higher than that of the rest of the biocatalysts). To analyze if this behavior can depend on the used raw material, the specific activity of the biocatalysts was determined using soybean oil, waste frying oil, acid oil from soybean soapstock, and *Jatropha hieronymi* oil. Soybean oil is one of the main oils to produce biodiesel in Argentina [30] while the used frying oils, which have low value as food but high energy content, are a domestic and gastronomic industry scrap. Then, biodiesel production from waste frying oils could be a sustainable alternative to reduce the price of biofuel [31]. The acid oil from soapstock is a side-product generated during soybean oil purification. This contains a large amount of free fatty acids (50-80wt% of FFA approx.), and a mixture of phospholipids, tocopherols, sterols, degraded and oxidized components, pigments, salts, color bodies, triglycerides, diglycerides, and monoglycerides in a minor proportion [32]. Converting this acid oil into biodiesel could give it greater added value.

On the other hand, *Jatropha hieronymi* is an endemic and non-conventional oilseed species from the semiarid and arid northwest of Argentina with an oil concentration of approx. 36 wt%. This oil has a 4,07 wt% of FFA and is presumably toxic [33,34]. Then, it does not represent competition with agricultural food crops and diversifies farmland. For these reasons, it also has economic potential as an alternative feedstock to produce biofuels [34].

As it is shown in Table 2, when the support is modified with metals, its specific activity increases between 1,07 to 1,35 times depending on the oils employed. Meanwhile, the LOBE specific activity was 6,81 to 10,70 times higher than that of $L_{PF}/SBA-15$, presenting the best specific activity for all used raw materials. The question is: why the lipase from *Pseudomonas fluorescens* shows greater activity when is immobilized by biosilicification.

Table 2. Comparison of the biocatalysts specific activity for the different raw materials used.

	Raw material	$L_{PF}/SBA-15$	$L_{PF}/Ca/SBA-15$	$L_{PF}/Na/SBA-15$	LOBE
Specific activity (U/g lipase)	Sunflower oil	0,92	1,24	1,24	7,29
	Soybean oil	0,88	1,14	1,00	6,51
	Frying waste oil	0,94	1,20	1,23	6,41
	Acid oil from soapstock	0,64	0,88	1,02	6,85
	J. Hieronymi oil	0,99	1,06	1,16	6,55

In general, when a chemical transformation takes place in a porous catalytic material, the overall process involves the following steps: 1) diffusion of reagents from within the fluid phase towards the external surface of the catalytic support, 2) diffusion of reactants through the pores of the catalyst, 3) adsorption of reagents, 4) surface reaction, 5) desorption of products, 6) diffusion of the products through the pores towards the outside of the material, 7) diffusion of the products from the external surface of the material into the surrounding fluid. Steps 3, 4, and 5 correspond to the chemical transformation and would be similar for the different biocatalysts. In the other stages, two important diffusion processes occur: (a) the mass transfer between the outer surface of the catalyst and the fluid, and (b) the mass transport inside the pores of the catalyst. The diffusion of reactants and products within

pores is strongly influenced by confinement effects in the mesoporous structure. Thus, LOBE structure consisting in interconnected channels and cavities that allow the communication or access to various pores within the structure could be responsible for its higher specific activity [35]. The use of materials with three-dimensional porous networks results advantageous because this pore structure provides better availability of active sites and lower pore-blocking [36]. Likewise, this three-dimensional pore architecture of LOBE (Figure 2) would favor mass transfer, promoting mixing of substrates and interaction with lipase owing cross flow; meanwhile the unidirectional pore system of SBA-15 only lead to an one dimensional flow that does not promote mixing of the substrates (Figure 4) [37].

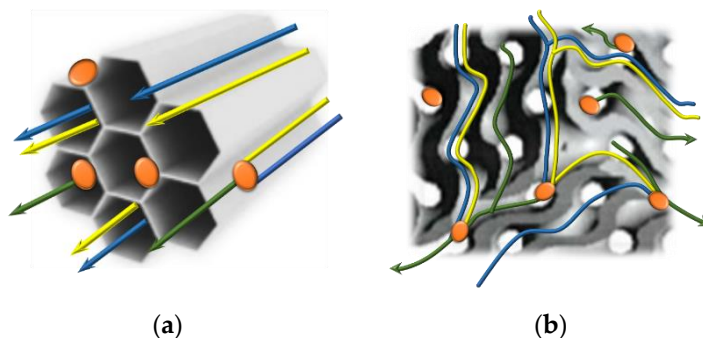


Figure 4. Schematic representation of substrate mixtures and interaction with lipase immobilized on different supports: (a) SBA-15, (b) LOBE. Yellow flux: oil, light blue flux: alcohol, green flux: biodiesel, orange: immobilized lipase enzyme.

Funding: This research was funded by ANPCyT, CONICET-FYPF, and UTN through the following respective grants: PICT-2016-0472, PIO 13320150100014CO, and PID UTN5157.

Acknowledgments: All authors are members of the research career of the Argentinian Research Council (CONICET). They would like to thank CONICET, FONCyT, MINCyT-Cba, and UTN-FRC for financial support. The authors also thank J.D. Fernández for assistance with surface area measurements.

References

References must be numbered in order of appearance in the text (including citations in tables and legends) and listed individually at the end of the manuscript. We recommend preparing the references with a bibliography software package, such as EndNote, ReferenceManager or Zotero to avoid typing mistakes and duplicated references. Include the digital object identifier (DOI) for all references where available.

Citations and references in the Supplementary Materials are permitted provided that they also appear in the reference list here.

In the text, reference numbers should be placed in square brackets [] and placed before the punctuation; for example [1], [1–3] or [1,3]. For embedded citations in the text with pagination, use both parentheses and brackets to indicate the reference number and page numbers; for example [5] (p. 10), or [6] (pp. 101–105).

1. R.A. Sheldon, J.M. Woodley, Role of Biocatalysis in Sustainable Chemistry, *Chem. Rev.* 118 (2018) 801–838. doi:10.1021/acs.chemrev.7b00203.
2. A. Hagen, S. Poust, T. De Rond, J.L. Fortman, L. Katz, C.J. Petzold, J.D. Keasling, Engineering a Polyketide Synthase for in Vitro Production of Adipic Acid, *ACS Synth. Biol.* 5 (2016) 21–27. doi:10.1021/acssynbio.5b00153.
3. Z. Liu, F.H. Arnold, New-to-nature chemistry from old protein machinery: carbene and nitrene transferases, *Curr. Opin. Biotechnol.* 69 (2021) 43–51. doi:10.1016/j.copbio.2020.12.005.
4. R.A. Sheldon, S. Van Pelt, Enzyme immobilisation in biocatalysis: why, what and how, *Chem. Soc. Rev.* 42 (2013) 6223–6235. doi:10.1039/c3cs60075k.
5. A. Salis, M.S. Bhattacharyya, M. Monduzzi, V. Solinas, Role of the support surface on the loading and the activity of *Pseudomonas fluorescens* lipase used for biodiesel synthesis, *J. Mol. Catal. B Enzym.* 57 (2009) 262–269. doi:10.1016/j.molcatb.2008.09.015.
6. G.O. Ferrero, H.J. Rojas, C.E. Argaraña, G.A. Eimer, Towards sustainable biofuel production: Design of a new biocatalyst to biodiesel synthesis from waste oil and commercial ethanol, *J. Clean. Prod.* 139 (2016) 495–503. doi:10.1016/j.jclepro.2016.08.047.

7. D.N. Tran, K.J. Balkus, Perspective of Recent Progress in Immobilization of Enzymes, *ACS Catal.* 1 (2011) 956–968. doi:10.1021/cs200124a.
8. G.O. Ferrero, E.M. Sánchez-Faba, G.A. Eimer, Two products one catalyst: Emulsifiers and biodiesel production combining enzymology, nanostructured materials engineering and simulation models, *Chem. Eng. J.* 348 (2018) 960–965. doi:10.1016/j.cej.2018.05.048.
9. I. Itabaiana, F.K. Sutili, S.G.F. Leite, K.M. Gonçalves, Y. Cordeiro, I.C.R. Leal, L.S.M. Miranda, M. Ojeda, R. Luque, R.O.M.A. de Souza, Continuous flow valorization of fatty acid waste using silica-immobilized lipases, *Green Chem.* 15 (2013) 518–524. doi:10.1039/c2gc36674f.
10. L. Zhong, Y. Feng, G. Wang, Z. Wang, M. Bilal, H. Lv, S. Jia, J. Cui, Production and use of immobilized lipases in/on nanomaterials: A review from the waste to biodiesel production, *Int. J. Biol. Macromol.* 152 (2020) 207–222. doi:10.1016/j.ijbiomac.2020.02.258.
11. R. Luque, J.C. Lovett, B. Datta, J. Clancy, J.M. Campelo, A.A. Romer, Biodiesel as feasible petrol fuel replacement: a multidisciplinary overview, *Energy Environ. Sci.* 3 (2010) 1706–1721. doi:10.1039/c0ee00085j.
12. H. Zhang, H. Li, C.C. Xu, S. Yang, Heterogeneously Chemo/Enzyme-Functionalized Porous Polymeric Catalysts of High-Performance for Efficient Biodiesel Production, *ACS Catal.* 9 (2019) 10990–11029. doi:10.1021/acscatal.9b02748.
13. R. Jambulingam, M. Shalma, V. Shankar, Biodiesel production using lipase immobilised functionalized magnetic nanocatalyst from oleaginous fungal lipid, *J. Clean. Prod.* 215 (2019) 245–258. doi:10.1016/j.jclepro.2018.12.146.
14. F. Esmi, T. Nematian, Z. Salehi, A.A. Khodadadi, A.K. Dalai, Amine and aldehyde functionalized mesoporous silica on magnetic nanoparticles for enhanced lipase immobilization, biodiesel production, and facile separation, *Fuel.* 291 (2021) 120126. doi:10.1016/j.fuel.2021.120126.
15. D. Zhao, Q. Huo, J. Feng, B.F. Chmelka, G.D. Stucky, Nonionic Triblock and Star Diblock Copolymer and Oligomeric Surfactant Syntheses of Highly Ordered, Hydrothermally Stable, Mesoporous Silica Structures, *J. Am. Chem. Soc.* 120 (1998) 6024–6036. doi:10.1021/ja974025i.
16. V. Elías, E. Vaschetto, K. Sapag, M. Oliva, S. Casuscelli, G. Eimer, MCM-41-based materials for the photo-catalytic degradation of Acid Orange 7, *Catal. Today.* 172 (2011) 58–65. doi:10.1016/j.cattod.2011.05.003.
17. G.O. Ferrero, E.M.S. Faba, G.A. Eimer, Biodiesel production from alternative raw materials using a heterogeneous Low Ordered Biosilicified Enzyme as biocatalyst, *Biotechnol. Biofuels.* 14 (2020) 1–11. doi:10.21203/rs.3.rs-23390/v1.
18. M.M. Bradford, A rapid and sensitive method for the quantitation of microgram quantities of protein utilizing the principle of protein-dye binding, *Anal. Biochem.* 72 (1976) 248–254. doi:10.1016/0003-2697(76)90527-3.
19. G.O. Ferrero, E.M. Sánchez Faba, A.A. Rickert, G.A. Eimer, Alternatives to rethink tomorrow: Biodiesel production from residual and non-edible oils using biocatalyst technology, *Renew. Energy.* 150 (2020) 128–135. doi:10.1016/j.renene.2019.12.114.
20. M.S. Carvalho, M.A. Mendonça, D.M.M. Pinho, I.S. Resck, P.A.Z. Suarez, Chromatographic analyses of fatty acid methyl esters by HPLC-UV and GC-FID, *J. Braz. Chem. Soc.* 23 (2012) 763–769. doi:10.1590/S0103-50532012000400023.
21. A. Salis, M.F. Casula, M.S. Bhattacharyya, M. Pinna, V. Solinas, M. Monduzzi, Physical and Chemical Lipase Adsorption on SBA-15: Effect of Different Interactions on Enzyme Loading and Catalytic Performance, *ChemCatChem.* 2 (2010) 322–329. doi:10.1002/cctc.200900288.
22. S. Cebrián-García, A. Balu, A. García, R. Luque, Sol-Gel Immobilisation of Lipases: Towards Active and Stable Biocatalysts for the Esterification of Valeric Acid, *Molecules.* 23 (2018) 2283–2296. doi:10.3390/molecules23092283.
23. C. Morhardt, B. Ketterer, S. Heißler, M. Franzreb, Direct quantification of immobilized enzymes by means of FTIR ATR spectroscopy - A process analytics tool for biotransformations applying non-porous magnetic enzyme carriers, *J. Mol. Catal. B Enzym.* 107 (2014) 55–63. doi:10.1016/j.molcatb.2014.05.018.
24. F. Dousseau, M. Pezolet, Determination of the secondary structure content of proteins in aqueous solutions from their amide I and amide II infrared bands. Comparison between classical and partial least-squares methods, *Biochemistry.* 29 (1990) 8771–8779. doi:10.1021/bi00489a038.
25. H. Sun, J. Han, Y. Ding, W. Li, J. Duan, P. Chen, H. Lou, X. Zheng, One-pot synthesized mesoporous Ca/SBA-15 solid base for transesterification of sunflower oil with methanol, *Appl. Catal. A Gen.* 390 (2010) 26–34. doi:10.1016/j.apcata.2010.09.030.
26. T.M. Albayati, A.M. Doyle, Encapsulated heterogeneous base catalysts onto SBA-15 nanoporous material as highly active catalysts in the transesterification of sunflower oil to biodiesel, *J. Nanoparticle Res.* 17 (2015) 109–119. doi:10.1007/s11051-015-2924-6.
27. I. Delfino, M. Portaccio, B. Della Ventura, D.G. Mita, M. Lepore, Enzyme distribution and secondary structure of sol-gel immobilized glucose oxidase by micro-attenuated total reflection FT-IR spectroscopy, *Mater. Sci. Eng. C.* 33 (2013) 304–310. doi:10.1016/j.msec.2012.08.044.
28. M. Portaccio, B. Della Ventura, D.G. Mita, N. Manolova, O. Stoilova, I. Rashkov, M. Lepore, FT-IR microscopy characterization of sol-gel layers prior and after glucose oxidase immobilization for biosensing applications, *J. Sol-Gel Sci. Technol.* (2011). doi:10.1007/s10971-010-2343-1.
29. A. Salis, M. Pinna, M. Monduzzi, V. Solinas, Comparison among immobilised lipases on macroporous polypropylene toward biodiesel synthesis, *J. Mol. Catal. B Enzym.* 54 (2008) 19–26. doi:10.1016/j.molcatb.2007.12.006.
30. D. Sigaudo, E. Terre, El mercado mundial de aceites vegetales: situación actual y perspectivas, *Bols. Comer. Rosario.* (2018) 6–8.

31. [31] I.L. García, Feedstocks and challenges to biofuel development, in: R. Luque, C.S. Ki Lin, K. Wilson, J. Clark (Eds.), *Handb. Biofuels Prod.*, Second Edi, Elsevier, Amsterdam, 2016: pp. 85–118. doi:10.1016/B978-0-08-100455-5.00005-9.
32. [32] J. Van Gerpen, G. Knothe, Bioenergy and Biofuels from Soybeans, in: L.A. Johnson, P.J. White, R. Galloway (Eds.), *Soybeans Chem. Prod. Process. Util.*, First edit, Urbana, 2008: pp. 499–538. doi:10.1016/B978-1-893997-64-6.50019-6.
33. [33] E.M. Sánchez Faba, G.O. Ferrero, J.M. Dias, G.A. Eimer, Alternative Raw Materials to Produce Biodiesel through Alkaline Heterogeneous Catalysis, *Catalysts*. 9 (2019) 690–704. doi:10.3390/catal9080690.
34. [34] A. Aranda-Rickert, L. Morzán, S. Fracchia, Seed oil content and fatty acid profiles of five Euphorbiaceae species from arid regions in Argentina with potential as biodiesel source, *Seed Sci. Res.* 21 (2011) 63–68. doi:10.1017/S0960258510000383.
35. [35] E.E. Gonzo, Conceptos Basicos Sobre Los Fenomenos En Catalisis Heterogenea, 2010. <http://www.ing.unsa.edu.ar/docs/librogonzo2011.pdf>.
36. [36] M. Falahati, A.A. Saboury, A. Shafiee, L. Ma'Mani, A.A. Moosavi-Movahedi, Immobilization of superoxide dismutase onto ordered mesoporous silica nanoparticles and improvement of its stability, *J. Iran. Chem. Soc.* 9 (2012) 157–161. doi:10.1007/s13738-011-0041-8.
37. [37] K. Schumacher, P.I. Ravikovitch, A. Du Chesne, A. V Neimark, K.K. Unger, Characterization of MCM-48 Materials, (2000). doi:10.1021/la991595i.